Journal of Power Technologies 100 (4) (2020) 341–350

Control Input Limited Switched Reluctance Motor with Auxiliary Sliding Mode Position Tracking Control

Chuansheng Tang[1], Gang Zhang[2], Jie Yang[3]✉, and Tao Li[4]

[1] Nanyang Institute of Technology, Henan Province, 473004, China
[2] Nanyang explosion proof Electrical Research Institute, Henan Province, 473004, China
[3] Henan Institute of Technology, Henan Province, 453000, China
[4] Department of Informatics, University of Zurich, Zurich, 8050, Switzerland
✉ yangtj56@163.com

Abstract

The drive system of a switched reluctance motor (SRM) is a nonlinear one with coupling between the rotor position, inductance, and flux linkage. Moreover, the system parameters change with the external environment such as temperature, humidity, and pressure. At the same time, uncertain factors including friction, torque fluctuation, and external interference in the system, reduce system stability and reliability. To effectively improve the influence of uncertain factors on the performance of an SRM system, this study proposes an auxiliary sliding position tracking method, under the condition of limited control input. First, the mathematical model of the system was established according to the structure and characteristics of an SRM. Second, an auxiliary sliding mode position tracking controller was designed by constructing the auxiliary system and utilizing the sliding mode control theory. Finally, the effectiveness and superiority of the proposed method were verified through comparison with proportional integral differential (PID) control and the traditional sliding mode control using simulation. Results demonstrate that under limited control input, the auxiliary sliding position tracking control method still delivers rapid and error-free tracking of the position and speed for the change of model parameters. The recommended scheme has a response time 2.9 times shorter than that of PID control. Furthermore, the steady-state errors of the PID control position and speed are 0.66 rad and 1.62 rad/s, respectively. The control input of the traditional sliding mode control has greater chattering than the proposed method. When the system has interference, the designed method under the condition of limited control input can achieve the desired tracking command within 1.7 s. The steady-state error is 0.0044 rad, and the steady-state accuracy of the developed scheme is 10.3 times higher than that of PID control. Therefore, the proposed method enjoys both high position tracking accuracy and strong robustness to external disturbances.

Keywords: switched reluctance motor, auxiliary system, sliding mode control, position tracking

1 Introduction

The switched reluctance motor (SRM) is similar to the reactive stepping motor and is a kind of doubly salient pole variable reluctance motor. The salient poles of an SRM's stator and rotor are made of silicon steel sheets with high permeability. The rotor has no winding or permanent magnet. The stator pole is surrounded by concentrated winding, whereas the $2q$ pole windings of π/q space angle between the stator winding are in series or in parallel and form phase winding. The SRM follows the principle of minimum reluctance to ensure that the flux is always closed along the path with minimum reluctance. The characteristics of the SRM include: rigid structure, high reliability and robustness, the lack of a permanent magnet, fast dynamic response and low manufacturing cost. Moreover, the speed control system of the SRM has the advantages of a traditional alternating current and a direct current (DC) speed control system. Therefore, the SRM shows strong market competitiveness in traction transportation, electric vehicles, general industry, the aviation industry, household appliances, high-speed motors and servo control systems, among others.

Given the increasing demand for SRM applications, the design, production, and application of SRM are studied. As regards design, this study mainly aims at addressing the non-linearity of the SRM's internal magnetic field and the difficulty of analyzing the phase current waveform caused by the non-linear switching power supply. Furthermore, this work explores the analysis and accurate calculation of the SRM electromagnetic torque [1, 2]. The SRM is widely used in precision manufacturing, blowers, compressors, turbochargers and flywheels for high-speed applications [3]. The study of SRM also focuses on electric vehicles in low speed uses [4]. The SRM rotor consists only of low loss silicon steel and stator winding without a permanent magnet, thereby reducing the

manufacturing cost and maintaining good mechanical and thermal stability [5]. Consequently, the said motor is highly suitable for application in hybrid vehicles.

However, the dynamic model of the SRM drive system is difficult to establish accurately. The model has the characteristics of nonlinear, strong coupling, multivariable and multi parameters, thereby increasing the difficulty of system control [6]. Second, the SRM stator winding is embedded in the cogging, and the cogging effect will cause torque fluctuation on the rotor [7]. Moreover, with the complexity of the working environment, the factors of parameter uncertainty, load disturbance, thrust fluctuation, and friction further increase the difficulty of control system design in SRM systems [8]. Actual control of the SRM system is always limited by certain conditions, including the control input torque or current of the motor speed loop design that cannot be greater than its rated value. Therefore, controlling the SRM with multiple constraints under the condition of limited control input is more practical.

2 State of art

The SRM involves many complex factors, such as strong coupling, nonlinearity, and multi-time variation. To effectively improve the influence of these factors on system performance and deliver high-performance dynamic control of the motor under the constraints of multiple factors, the SRM has become a research hotspot. Proportional integral differential (PID) control with fixed gain is widely used in industry because of its simple structure. To ensure the constant current of a rotating high temperature superconductivity (HTS) flux pump excitation coil, Jeon et al. [9] controlled the magnetic field of the electromagnet by means of fixed gain PID. The authors successfully compensated for the change of HTS coil current under the condition of changing the speed and direction and achieved constant current output. However, the PID control parameters were fixed. Moreover, performance of the system deteriorated significantly when the internal characteristics of the system changed or external disturbance altered considerably, indeed to such an extent that system instability and even collapse occurred. Accordingly, Angel et al. [10] introduced a fractional order operator into PID control. That operator increased the degree of freedom of design and was applied to the motor generator speed control system. The proposed fractional order PID control had strong robustness to parameter changes, but the resulting method relying on the system model was robust to small-scale disturbances. Consequently, its application was limited.

To make the PID control gain automatically adjust with the changes of the system model parameters and disturbances, He et al. [11] combined fuzzy theory with PID control and applied it to SRM control, thereby effectively reducing the large torque fluctuation and enhancing the anti-interference ability of the system. However, the number of fuzzy rules, which increased the complexity of the system, made calculations difficult. Adaptive control improved the influence of model parameter changes on system performance by supplying online identification of system model parameters - and this method was still in accordance with the system model [12]. Online parameter estimation increased the calculation of the system and consequently reduced the dynamic response ability of the system. Adaptive control was often combined with sliding mode control and backstepping control. In the$\alpha\beta$ static coordinate system, Tang et al. [13] estimated the stator current of linear motor online through the sliding mode observer and estimated the position and speed of the actuator by using the back EMF model. This technique effectively avoided the influence of external disturbance on the speed and position estimation accuracy of the actuator, but exhibited strong dependence on stator resistance. To improve the chattering phenomenon caused by the traditional sliding mode control, Nihad et al. [14] designed a load disturbance observer to compensate and effectively improved the dynamic performance of the motor system. This approach had high estimation accuracy in high-speed operation but showed large error in low-speed operation, thereby limiting its application. Ali et al. [15] proposed a dynamic sliding mode control method based on an integral observer for uncertain induction in motor drive systems. The introduction of an integral observer improved the chattering phenomenon, increased the complexity of controller design and reduced the reliability of the system to a certain extent. Abdelkader et al. [16] combined adaptive and backstep control to reverse design the system for an uncertain DC motor speed control scheme, but this system required multiple derivatives, including a calculation explosion problem caused by the derivation. Therefore, the proposed method should be combined with other techniques. Tang et al. [17] produced an integrated design of speed, thrust and flux loops through adaptive backstepping control, but a computational explosion still ensued. Using the port-controlled Hamiltonian model of a bearingless switched reluctance motor (BSRM) rotor mechanical subsystem, Chen et al. [18] designed a passive controller of the BSRM rotor mechanical subsystem using the interconnection and damping assignment passive control method and adding integral links, devel-

oped a control performance evaluation function with an energy function, and optimized the controller parameters by using a cuckoo search algorithm, so that the system enjoyed high steady-state accuracy and fast dynamic response ability. This method depended heavily on the resistance, inductance, and other parameters of the motor. Mohamed et al. [19] applied predictive control to an induction motor and proposed a sensorless direct torque predictive control technique which used the extended Kalman filter as the driver to estimate the state of the motor model. The control method effectively reduced flux and torque ripple, but the prediction of the system state variables required prior and model parameter data. Furthermore, the size of the predictive control sample data had a significant impact on system accuracy. Masoudi et al. [20] used applied fuzzy estimation to achieve automatic gain adjustment of the sliding mode control. Their method involved the self-learning ability of fuzzy control and the insensitivity of the sliding mode control to time-varying parameters, and also improved the chattering of the system. Nevertheless, the chattering phenomenon persisted, thereby affecting the performance of the system. Xu et al. [21] combined a single neuron with an adaptive method to realize position tracking control of a linear SRM, the on-line estimation of controller gain by neuron, and on-line automatic adjustment of neuron weight by using the Drosophila optimization algorithm. This approach had strong robustness and anti-interference ability, but its structure was complex and its application in engineering would be difficult. To reduce the chattering phenomenon caused by the sliding mode control, Tang et al. [22] improved the dynamic performance of the system, effectively by introducing a nonlinear disturbance observer to monitor and compensate for the unmodeled dynamic and external disturbance of the system. The accuracy of the observer still depended on the model parameters of the system, so meeting the requirements of high accuracy occasions was challenging. Zhao et al. [23] proposed a fuzzy backstepping position motor control method according to the observer. The reduced order observer was applied to estimate rotor angular velocity. The fuzzy logic system was employed to approach the unknown nonlinearity in the system model, while the problem of calculation explosion in backstepping design was solved by dynamic surface control. This proposed method effectively improved the tracking accuracy and dynamic performance of the system and has good start-up performance and reliability. However, this approach was complex and difficult in practical application.

For an actual motor system, whether for position, speed or current control, the total amount of control input cannot be infinite. That system usually needed to be designed under a rated state, such as rated torque, voltage, or current. Conversely, the study of the above control method rarely involved the consideration of a saturation limit. In fact, the existence of control input saturation constraints inevitably affected the dynamic performance of the system. Therefore, examining the multi-factor constraints control method of the SRM with control input saturation constraints is more practical.

According to the above review, a position control method of the SRM based on the auxiliary sliding mode was proposed. Considering the constraints of the control input, an auxiliary system was developed to compensate for the changes of model parameters and external disturbances. The suggested approach improved the robustness and tracking ability of the system and provided high-performance position tracking control of the SRM.

The remainder of this study is organized as follows. Section 3 describes the structure of the SRM and deals with the building of the dynamic SRM model and design of the auxiliary sliding position controller to analyze model stability. Section 4 verifies the effectiveness and superiority of the proposed method through numerical simulation analysis and comparison of the auxiliary sliding control method. Section 5 summarizes the conclusions of this work.

3 Methodology

3.1 Structure and mathematical model of the SRM

The structure of the linear SRM in this study is shown in Figure 1. The motor is a three-phase 6/4 SRM with six stator poles and four rotor poles.

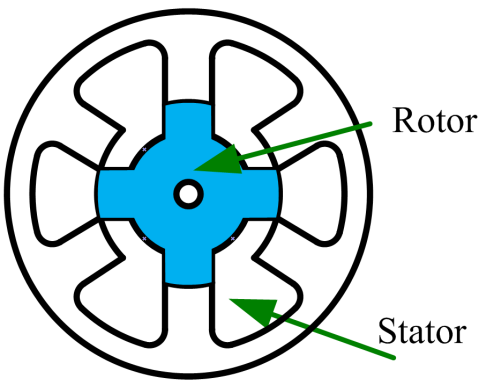

Figure 1: Structure model of the SRM

To simplify the analysis, the SRM meets the following conditions:

(1) The DC bus voltage of main circuit is constant.

(2) The power electronic switch device is an ideal switch. Hence, the voltage is zero when the device is turned on and the current is zero when it is turned off. Moreover, no delay occurs in turning the device on and off.

(3) The close hysteresis and eddy current effect are overlooked: iron loss is disregarded.

(4) The parameters of each phase are symmetrical, two windings of each phase are connected in series, and mutual inductance between the phases is ignored.

(5) In a period of current pulsation, the speed is constant.

Under the above assumptions, the mathematical model of SRM control can be expressed as follows.

Voltage equation is:

$$U_k = R_k i_k + \frac{\mathrm{d}}{\mathrm{dt}}$$

Torque expression is:

$$T_m = \sum_{k=1}^{3} \frac{\partial \lambda_k(x,i)}{\partial x} i_k$$

The equation of motion is:

$$T_m = J_n\ddot{\theta} + B_n\dot{\theta} + T_L + T_f + T_r$$

where U_k, i_k, ψ_k and R_k indicate the phase voltage, phase current, phase flux, and phase resistance, respectively. J_n is the mass of the rotor. θ suggests the position of the rotor. $\dot{\theta} = \omega$ represents the angular speed of the rotor. T_m signifies the electromagnetic torque. B_n is the linear friction coefficient. T_r, T_L and T_f denote the torque fluctuation, load disturbance and nonlinear friction torque of the system, respectively.

Considering the change of parameters in the system, Eq. (3) can be expressed as follows:

$$T_m = J_n\ddot{\theta} + B_n\dot{\theta} + J\ddot{\theta} + B\dot{\theta} + T_L + T_f + T_r$$

where J represents the uncertainty term of the kinematical massJ_n. B is the uncertainty term of the linear friction coefficient B_n.

3.2 Control objectives

If $x = \theta$ and $x_2 = \dot{x}_1 = \dot{\theta}$, then Eq. (4) can be expressed as follows:

$$\begin{cases} \dot{x}_1 = x_2 \\ \dot{x}_1 = f(x,t) + \mathrm{bu} + \mathrm{dt} \end{cases}$$

where $b = 1/J_n$, and $f(x,t) = -B_n/J_n$. dt $= -(J\ddot{\theta} + B\dot{\theta} + T_L + T_f + T_r)/J_n$is the total uncertainty of the system and Eq. (4) meets$\|\mathrm{dt}\| \leq D$. u is the limited control quantity. The hypothesis suggests that the maximum control input value is $u_{\max} > D$, $u = u - \nu$ and $u = \mathrm{sat}(\nu)$. The control input saturation function can be expressed as follows:

$$\mathrm{sat}(\nu) = \begin{cases} u_{\max}, & \nu > u_{\max} \\ \nu, \|\nu\| \leq u_{\max} \\ -u_{\max}, \nu < -u_{\max} \end{cases}$$

Under the condition of limited input control, the goal of the control is to design the control input u when the system has parameter uncertainty and load disturbance, so that the system can achieve the expected position tracking θ_d and the expected angular speed tracking $\omega_d = \dot{\theta}_d$ of the motor rotor. That is, $\theta \to \theta_d$ and$\omega \to \omega_d$ when $t \to \infty$.

3.3 Design of the auxiliary sliding mode controller

A stable auxiliary error system is defined to design the sliding mode controller. The proposed controller structure is shown in Figure 2.

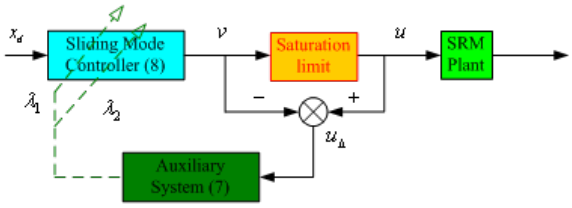

Figure 2: Auxiliary sliding mode controller of the SRM

The stable auxiliary system is expressed as

$$\begin{cases} \dot{\lambda}_1 = -c_1\lambda_1 + \lambda_2 \\ \dot{\lambda}_2 = -c_1\lambda_2 + b\lambda \end{cases}$$

To guarantee that $t \to \infty$,$\lambda_1 \to 0$ and $\lambda_2 \to 0$, only$c_1 > 0$ and $c_2 > 0$. Furthermore, to prevent the instability of Eq. (7) caused by too substantial u, the

condition thatc_1 and c_2 are large enough should be assured.

The defined position error is

$$e = x_1 - x_d - \lambda_1$$

Then, $\dot{e} = \dot{x}_1 - \dot{x}_d - \dot{\lambda}_1 = x_2 - \dot{x}_d - \dot{\lambda}_2 + c_1\lambda_1$.

The designed sliding surface is represented by $s = \dot{e} + \alpha\varepsilon + \beta e^{\frac{p}{q}}$, in which$a > 0$, $\beta > 0$,and $q > p > 0$, q and p are odd.

$$\begin{aligned}
&\dot{s} = \ddot{e} + \left(a + \beta\tfrac{p}{q}e^{\frac{p}{q}-1}\right)e = \ddot{x}_1 - \ddot{x}_d - \ddot{\lambda}_1 + \\
&\left(\alpha + \beta\tfrac{p}{q}e^{\frac{p}{q}-1}\right)(x_2 - \dot{x}_d - \lambda_2 + c_1\lambda_1) \\
&= f(x,t) + \mathrm{bu} + \mathrm{dt} - \ddot{x}_d - \left(-c_1\ddot{\lambda}_1 + \dot{\lambda}_2\right) + \\
&\left(\alpha + \beta\tfrac{p}{q}e^{\frac{p}{q}-1}\right)(x_2 - \dot{x}_d - \lambda_2 + c_1\lambda_1) = f(x,t) + \\
&\mathrm{bu} + \mathrm{dt} - \ddot{x}_d + c_1(-c_1\lambda_1 + \lambda_2) - (-c_2\lambda_2 + bu_\Delta) + \\
&\left(\alpha + \beta\tfrac{p}{q}e^{\frac{p}{q}-1}\right)(x_2 - \dot{x}_d - \lambda_2 + c_1\lambda_1) \\
&= f(x,t) + \mathrm{bv} + \mathrm{dt} - \ddot{x}_d - \alpha\dot{x}_d + c_1\left(\alpha + \beta\tfrac{p}{q}e^{\frac{p}{q}-1} - c_1\right)\lambda_1 + \\
&\left(c_1 + c_2 - \alpha - \beta\tfrac{p}{q}e^{\frac{p}{q}-1}\right)\lambda_2 + \left(\alpha + \beta\tfrac{p}{q}e^{\frac{p}{q}-1}\right)x_2
\end{aligned}$$

The controller can be designed as follows:

$$\begin{aligned}
\nu = &-\tfrac{1}{b}[f(x,t) - \ddot{x}_d - \alpha\dot{x}_d + c_1\left(\alpha + \beta\tfrac{p}{q}e^{\frac{p}{q}-1} - c_1\right)\lambda_1 + \\
&\left(c_1 + c_2 - \alpha - \beta\tfrac{p}{q}e^{\frac{p}{q}-1}\right)\lambda_2 + \left(\alpha + \beta\tfrac{p}{q}e^{\frac{p}{q}-1}\right)x_2 - \\
&\eta sgn(s)]
\end{aligned}$$

Eq. (10) is substituted into the sliding surface and $\dot{s} = \mathrm{dt} - \eta\sigma\gamma\nu(s)$ can be obtained.

The Lyapunov function is defined. That is, $V = 0.5s^2$. Consequently, $V = s\dot{s} = s(\mathrm{dt} - \eta\sigma\gamma\nu(s)) = \mathrm{dt}\cdot s - \eta|s| \le 0$.

The above analysis indicates that the effectiveness of the designed control method depends on whether or not the state of the auxiliary system$\lambda_1 \to 0$ and $\lambda_2 \to 0$ are valid, i.e. the boundedness of u. Under the initial condition, the boundedness of $V = 0.5s_0^2$ guarantees the boundedness of u. At other times, selecting the auxiliary system parameters c_1 and c_2 can guarantee the auxiliary system state $\lambda_1 \to 0$ and $\lambda_2 \to 0$ according to Eq. (7), so that $e \to 0$ and$\dot{e} \to 0$ can achieve $t \to 0$. V is bounded, i.e., u is bounded. Therefore, the tracking of the motor rotor position and angular velocity can be realized.

To improve the chattering phenomenon caused by the switching function of the conventional sliding mode control, the continuous hyperbolic tangent function is employed instead of the switching function. Then, the control input of the system can be expressed as follows:

$$\begin{aligned}
\nu = &-\tfrac{1}{b}[f(x,t) - \ddot{x}_d - \alpha\dot{x}_d + c_1\left(\alpha + \beta\tfrac{p}{q}e^{\frac{p}{q}-1} - c_1\right)\lambda_1 + \\
&\left(c_1 + c_2 - \alpha - \beta\tfrac{p}{q}e^{\frac{p}{q}-1}\right)\lambda_2 + \left(\alpha + \beta\tfrac{p}{q}e^{\frac{p}{q}-1}\right)x_2 - \\
&\eta\tanh\left(\tfrac{s}{\varepsilon}\right)]
\end{aligned}$$

where $\varepsilon > 0$, and its size determines the steepness of the hyperbolic tangent function. The expression of the hyperbolic tangent function is

$$tanh(x/\varepsilon) = \frac{e^{x/\varepsilon} - e^{-x/\varepsilon}}{e^{x/\varepsilon} + e^{-x/\varepsilon}}$$

4 Results analysis and discussion

To verify its effectiveness, the proposed method is compared with PID and the traditional sliding mode control.

The nominal parameters of the SRM model entails a rotor moment of inertia of $J_n = 8 \times 10^{-3}\mathrm{kg}\cdot m^2$, friction coefficient of $B_n = 0.2N\cdot m/s$, total system disturbance of dt $= 10$sint, $f(x,t) = -ax_2$, $a = B_n/J_n = 25$, and $a = 1/J_n = 125$. Then, the system model can be expressed as:

$$\begin{cases} \dot{x}_1 = x_2 \\ \dot{x}_1 = -25x_2 + 125u + \mathrm{dt} \end{cases}$$

The sampling period of the system is $T_s = 1$ms. The command signal of the rotor position is $x_1 = x_d =$ sint and the simulation study is divided into three working conditions.

4.1 Determination of the system model

When the system model is determined (i.e., no model parameter change and disturbance occurs), the simulation results are as shown from Figure 3 to Figure 8.

Figures 3 to 8 indicate that when the system does not experience model parameter change and disturbance, the following conclusions can be drawn: (1) PID control can deliver fast dynamic tracking of speed and position by adjusting the proportion, integral, and differential gain. When no control input saturation limit exists, the desired speed and position can be achieved in $0.3s$. When the control input saturation limit is ± 0.5nm, the speed and position tracking

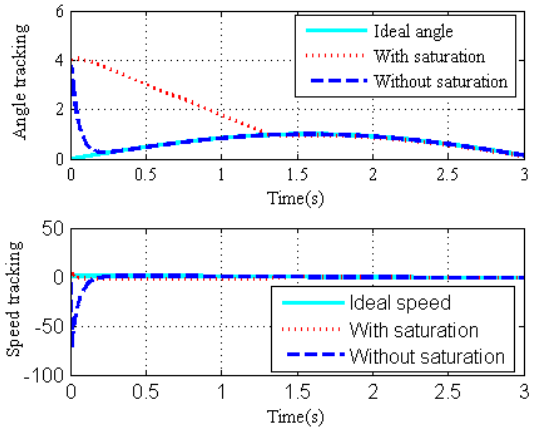

Figure 3: Response curves of the PID control angle and speed tracking

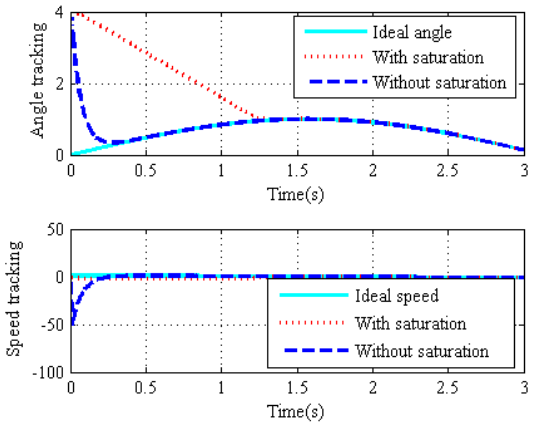

Figure 4: Response curves of the SMC control angle and speed tracking

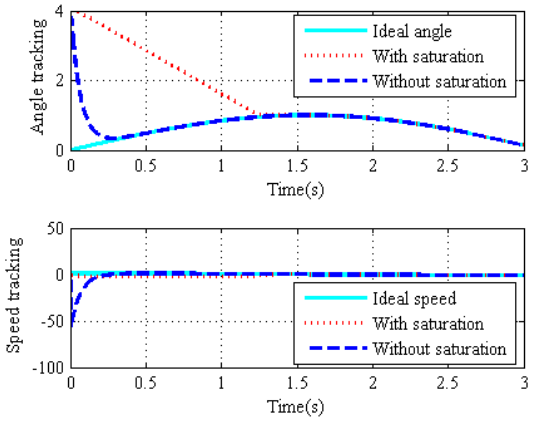

Figure 5: Response curves of the ASMC control angle and speed tracking

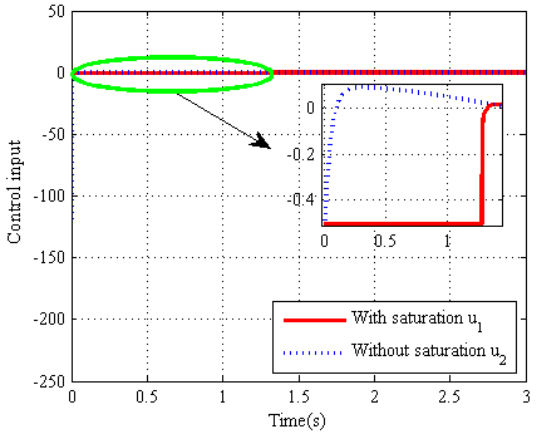

Figure 6: Response curve of the PID control input

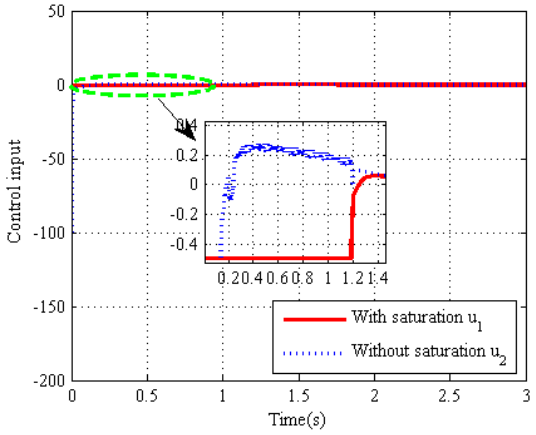

Figure 7: Response curve of the SMC control input

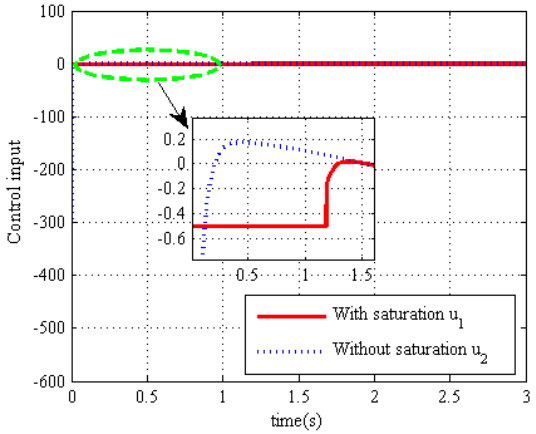

Figure 8: Response curve of the ASMC control input

need$1.4s$ for the corresponding time. (2) The sliding mode control has the same dynamic performance as

the proposed method and PID control. However, the input of the sliding mode control still has large chattering in the saturation limit stage. The input control of the proposed method remains smooth at this stage. This outcome arises from the effective improvement of the performance of the auxiliary system and the finite time sliding mode function.

4.2 Model parameter changes in the system

The simulation results for when the system has model parameter changes are shown in Figures 9 to 14.

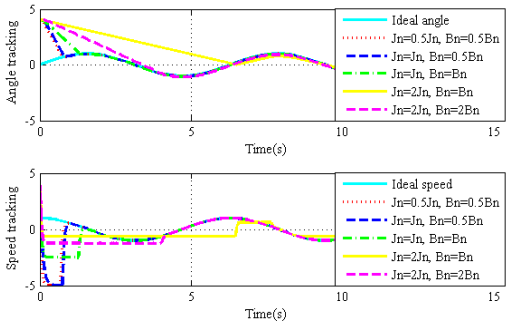

Figure 9: Response curves of the PID tracking

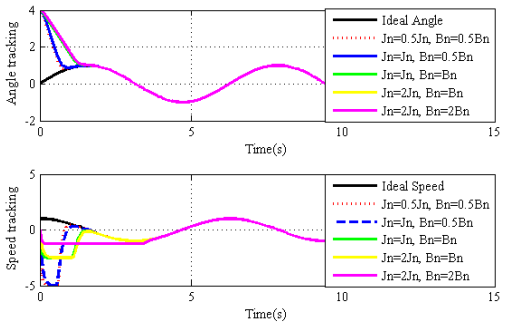

Figure 10: Response curves of the ASMC tracking

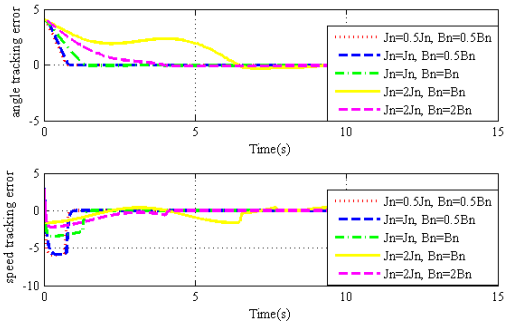

Figure 11: Response curves of the PID tracking error

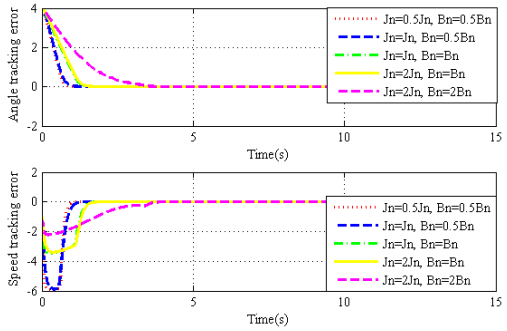

Figure 12: Response curves of the ASMC tracking error

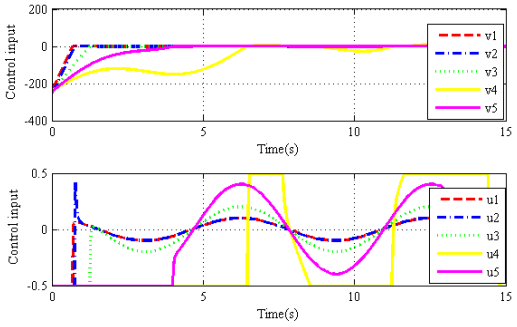

Figure 13: Response curves of the PID control input

Figures 9 to 14 show that the system model has parameter changes, and the following conclusions can be drawn: (1) For PID control, the rotor position and speed of the motor can achieve the desired command tracking when the model parameters are reduced. Furthermore, the response time changes from $1.4s$ to $1s$ before the parameter changes when the dynamic response ability is enhanced. However, a constant steady-state error of 0.03rad is present and the motor friction coefficient is constant. The moment of inertia doubles and the dynamic response time of PID control changes to $4.1s$. The position and speed of the motor have large steady-state errors of 0.66rad and0.62rad$/s$, respectively. (2) When the model parameters are reduced by half, the dynamic response ability of the proposed method is also significantly enhanced and the response time falls from $3.6s$ to $0.72s$. When the rotating inertia is doubled, the dynamic response ability remains unchanged. When the moment of inertia and the coefficient of viscous friction are doubled, the dynamic response time of the system changes from $1.4s$ to $1.8s$, thereby showing that the method has strong robust suppression ability for the

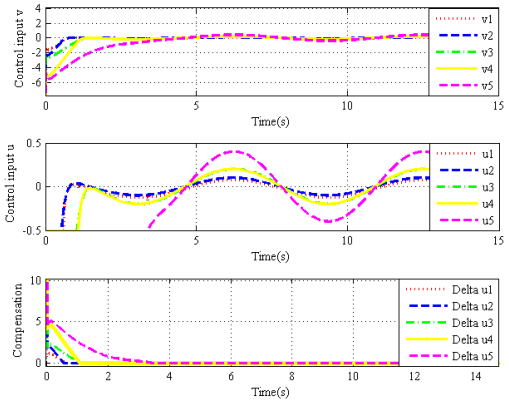

Figure 14: Response curves of the ASMC control input

parameter changes. (3) When the control input saturation is limited, the system starts with maximum torque (i.e., the saturation value of the control input) and the control input saturation limit will reduce the dynamic response ability of the system.

4.3 External disturbance in the system

The simulation of the system with an external disturbance is presented from Figures 15 to 17.

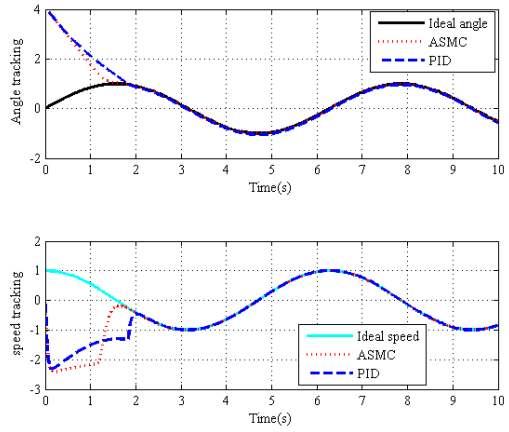

Figure 15: Response curves of the position tracking

Figures 15 to 17 show that when the system has external disturbance, the following conclusions can be drawn. (1) PID exhibits unsatisfactory starting performance, and 1.9s is needed to reach the steady state. Furthermore, a steady-state error of 0.045rad occurs. The proposed auxiliary sliding mode method achieves the expected tracking command in 1.7s, with

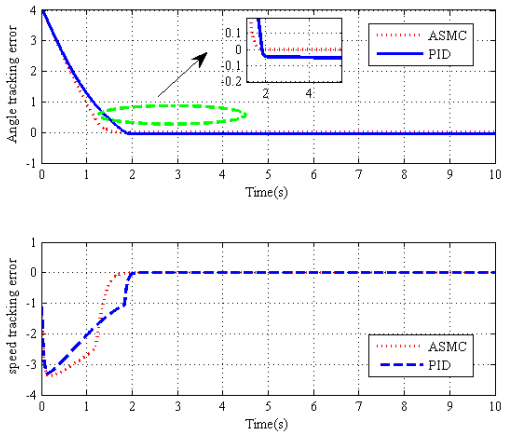

Figure 16: Response curves of the position tracking error

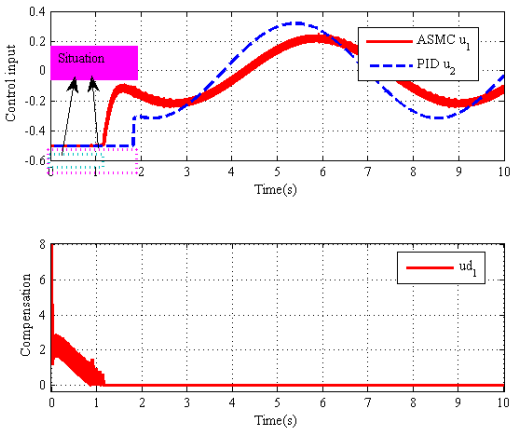

Figure 17: Response curves of the control input

a steady-state error of $4.4 \times 10^{-3} rad$. The steady-state precision increased by 10.3 times. (2) Figure 5(c) shows that the auxiliary sliding mode control possesses a compensation quantity in the saturation stage. This feature explains the higher dynamic response ability of the proposed technique than that of PID control. However, since the suggested approach still has large chattering when the system has a large disturbance, the disturbance observer for real-time observation and compensation should be combined to improve the performance of the system.

5 Conclusion

To effectively improve the influence of uncertain factors such as time-varying parameters and external disturbances on the control system accuracy of the SRM,

this study started with a mathematical SRM model and combined sliding mode control theory and the auxiliary system design method. Thus, a new SRM position control strategy was developed by combining theoretical derivation and numerical simulation. The following conclusions can be drawn:

(1) The designed method maintains high dynamic response and steady-state tracking performance under a limited control input when the system has time-varying parameters. The dynamic response time does not change considerably from 1.4s to 1.8s. The steady-state errors of the position and speed are $1.5 \times 10^{-10} rad$ and $2 \times 10^{-3} rad/s$, respectively. Conversely, PID control is sensitive to the change of the friction coefficient. When the friction coefficient of the motor is unchanged and the moment of inertia is doubled, the dynamic response time of PID control becomes 4.1s. Furthermore, and the position and speed of motor have large steady-state errors of 0.66*rad* and 1.62 *rad/s* , respectively.

(2) When the system has external interference, the designed method can achieve the desired tracking command within 1.7s under the condition of limited control input. The steady-state error is $4.4 \times 10^{-3} rad/s$ and the steady-state accuracy is 10.3 times higher than PID control.

(3) When no model parameters and disturbances occur, the designed method has a smoother control output than the traditional sliding mode control.

(4) Control input constraints will increase the response time and reduce the dynamic performance of the system.

According to the physical model of the SRM and with the combination of theory and numerical simulation, this study presents a rotor position tracking method that can effectively improve the parameter variation and external disturbance of the system. The proposed technique can meet the requirements of a high-speed and high-precision servo system and has certain application value. Given the limited experimental conditions, the suggested scheme requires further verification and control scheme optimization through subsequent experiments. In the design of this scheme, the physical model of the linear SRM ignores the influence of mutual inductance on the system (secondary factor). Using an experimental platform that considers the effect of this factor will achieve greater accuracy than the current methodology. At the same time, the proposed system should be combined with the observer method to improve the chattering of the system.

6 Acknowledgements

This study was supported by the Key Scientific Study Projects of Higher Education Institutions of Henan Province (Grant Nos. 20B470003 and 18B470007) and the Promotion Special Project of Scientific Study Program of Henan Province (Grant Nos. 202102210084 and202102210298).

References

[1] Y. Li, Q. Ma, and P. Xu. Improved general modelling method of SRMs based on normalised flux linkage. *Institution of Engineering and Technology Electric Power Applications*, 14(2):316–324, 2020.

[2] B. Howey, B. Bilgin, and A. Emadi. Design of a mutually coupled external-rotor direct drive E-bike switched reluctance motor. *Institution of Engineering and Technology Electrical Systems in Transportation*, 10(1):89–95, 2020.

[3] S. Li, S. Zhang, T. Habetler, and R. Harley. Modeling, design optimization, and applications of switched reluctance machines-a review. *IEEE Transactions on Industry Applications*, 55(3):2660–2681, 2019.

[4] E. Bostanci, M. Moallem, A. Parsapour, and B. Fahimi. Opportunities and challenges of switched reluctance motor drives for electric propulsion: a comparative study. *IEEE Transactions on Transportation Electrification*, 3(1):58–75, 2017.

[5] B. Burkhart, A. Klein-Hessling, I. Ralev, C. Weiss, and D.R. De. Technology, research and applications of switched reluctance drives. *CPSS Transactions on Power Electronics and Applications*, 2(1):12–27, 2017.

[6] S.G. Zuo, M.T. Liu, and S.L. Hu. Analytical modeling for inductance and torque of switched reluctance motor considering iron core magnetic saturation. *Journal of Xi'an Jiaotong University*, 53(7):118–125,143, 2019.

[7] S.G. Zuo, Y.P. Zheng, S.L. Hu, and Y. Mao. Analytical modeling of radial electromagnetic force for switched reluctance motor considering saturation effect. *Journal of Tongji University (Natural Science)*, 46(12):1736–1744, 2018.

[8] W. Ye, Q.W. Ma, P. Xu, and P.M. Zhang. Nonlinear fitting method for torque-angle characteristic model of switched reluctance motor. *Journal*

of Beijing University of Aeronautics and Astronautics, 45(1):83–92, 2019.

[9] H. Jeon, J. Lee, S. Han, J.H. Kim, C.J. Hyeon, H.M. Kim, H. Kang, T.K. Ko, and Y.S. Yoon. PID control of an electromagnet-based rotary HTS flux pump for maintaining constant field in HTS synchronous motors. *IEEE Transactions on Applied Superconductivity*, 28(4):1–5, 2018.

[10] L. Angel and J. Viola. Design and statistical robustness analysis of FOPID, IOPID and SIMC PID controllers applied to a motor-generator system. *IEEE Latin America Transactions*, 13(12):3724–3734, 2015.

[11] Y. He, Y. Tang, D. Lee, and J. Ahn. Suspending control scheme of 8/10 bearingless SRM based on adaptive fuzzy PID controller. *Chinese Journal of Electrical Engineering*, 2(2):60–67, 2016.

[12] A. Nguyen, M. Rafaq, H. Choi, and J.Jung. A model reference adaptive control based speed controller for a surface - mounted permanent magnet synchronous motor drive. *IEEE Transactions on Industrial Electronics*, 65(2):9399–9409, 2018.

[13] C. Tang, Y. Dai, and Y. Xiao. High precision position control of PMSLM using adaptive sliding-mode approach. *Journal of Electrical Systems*, 10(4):456–464, 2014.

[14] A. Nihad, U. Ateeq, A. Waqar, and M. Hamid. Disturbance observer based robust sliding mode control of permanent magnet synchronous motor. *Journal of Electrical Engineering and Technology*, 14(6):2531–2538, 2019.

[15] K. Ali, T. Hamed, and B. Oscar. Dynamic sliding mode position control of induction motors based load torque compensation using adaptive state observer. *Compel*, 37(6):2249–2262, 2018.

[16] H. Abdelkader, B. Houcine, C. Ilhami, and K. Korhan. Backstepping control of a separately excited DC motor. *Electrical Engineering*, 100(3):1393–1403, 2018.

[17] C. Tang and Z. Duan. Direct thrust - controlled PMSLM servo system based on back - stepping control. *IEEJ Transactions on Electrical and Electronic Engineering*, 13(5):785–790, 2018.

[18] L. Chen, H.H. Wang, J.W. Zhang, C. Tan, and Y. Wang. Optimization design of passivity - based controller for bearingless switched reluctance motor. *Journal of Guangxi University (Natural Science Edition*, 43(5):1756–1764, 2018.

[19] C. Mohamed, G. Amar, T. Med, and G. Noureddine. Senseless finite-state predictive torque control of induction motor fed by four-switch inverter using extended Kalman filter. *Compel*, 37(6):2006–2024, 2018.

[20] S. Masoudi, M.R. Soltanpour, and H. Abdollahi. A new adaptive fuzzy control method for a linear switched reluctance motor. *Institution of Engineering and Technology Electric Power Applications*, 12(9):1328–1336, 2018.

[21] K. Xu, C.S. Tang, J. Yang, J. Zhang, and J. Hu. Optimization of linear switched reluctance motor for single neuron adaptive position tracking control based on fruit fly optimization algorithm. *Journal of Engineering Science and Technology Review*, 13(1):160–165, 2020.

[22] C.S. Tang, Z.M. Li, and C. Li. Disturbance compensation based robust sliding - mode tracking control for uncertain robots. *Modular Machine Tool and Automatic Manufacturing Technique*, (7):99–101,104, 2016.

[23] E.L. Zhao, J.F. Yu, S. Cheng, and J.P. Yu. Observer - based fuzzy backstepping position tracking control for asynchronous motor stochastic system. *Motor and Control Application*, 47(1):8–14, 2020.